Chapter 5

SINGLE-MODE OPTOFLUIDIC DISTRIBUTED FEEDBACK DYE LASER

5.1 Introduction

Recently, several groups have demonstrated on-chip liquid dye lasers using different materials and laser cavity geometries [1-3]. Such lasers allow the integration of coherent light sources with other microfluidic and optical functionalities, and are of great interest for making fully functional "lab-on-a-chip" systems. However, the lack of both transverse mode and longitudinal mode selection in the previous demonstrations led to multiple mode operation and wide emission linewidths (~ 5 nm) that are hard to distinguish from amplified spontaneous emission (ASE). Balslev and Kristensen [4] recently demonstrated a microfluidic dye laser using a ~ 130th order Bragg grating imprinted on a glass substrate without transverse confinement. Approximately single spatial mode operation was observed due to the high losses of higher-order spatial modes. In this chapter we present, to our knowledge, the first chip-based single-mode liquid dye laser using a distributed feedback (DFB) structure. DFB cavities combined with 3D optical waveguides are very efficient structures for making single frequency microfabricated lasers [5]. Their implementation on a microfluidic chip will greatly improve the performance of microfabricated liquid dye lasers.

5.2 Chip design and fabrication of single mode DFB dye laser

The schematic diagram of our device is shown in Figure 5.1. The laser chip is entirely made of poly(dimethylsiloxane) (PDMS), a silicone elastomer which has become

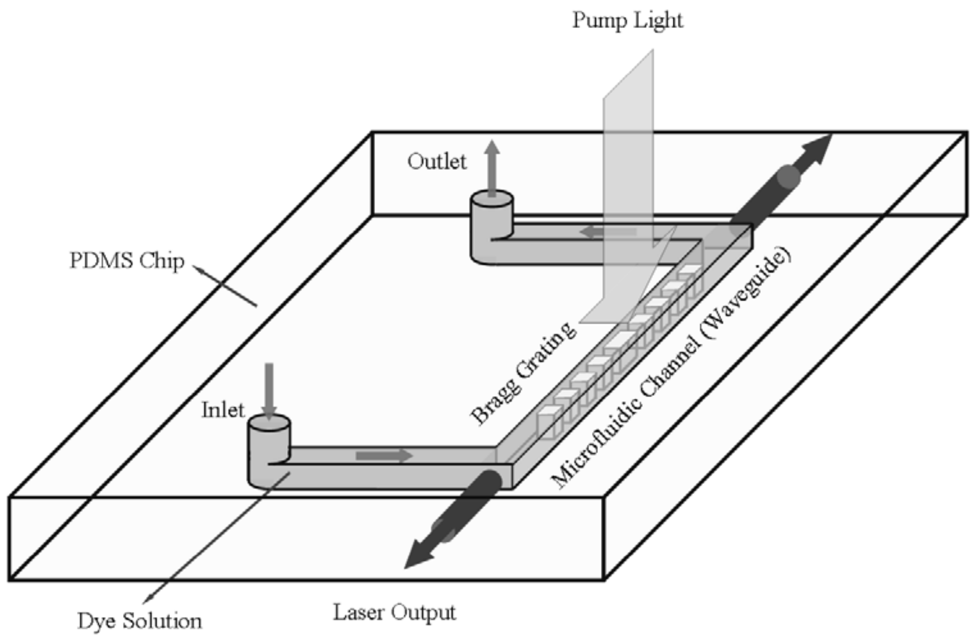

Figure 5.1. Schematic diagram of a monolithic optofluidic DFB dye laser

popular for microfluidics and nanofabrication [6, 7], and has good optical properties in the visible region. A sufficiently small microfluidic channel, when filled with a dye solution of higher refractive index than that of PDMS (n_{PDMS} = 1.406), acts as a single-mode optical waveguide. The gain medium is a 1 mM solution of Rhodamine 6G in a methanol and ethylene glycol mixture with refractive index of 1.409. The periodic PDMS posts inside the channel form a 4 mm long 15th order Bragg grating which provides the optical feedback necessary for the laser action. In addition, a 15π phase shift is introduced at the center of the grating to ensure single frequency operation. The PDMS posts also provide support for the microfluidic channel.

The fabrication of the optofluidic DFB dye laser uses the same replica molding soft lithography technique which is widely used to make microfluidic devices [8, 9]. Briefly, a master mold was fabricated using conventional photolithography. 2 μm thick

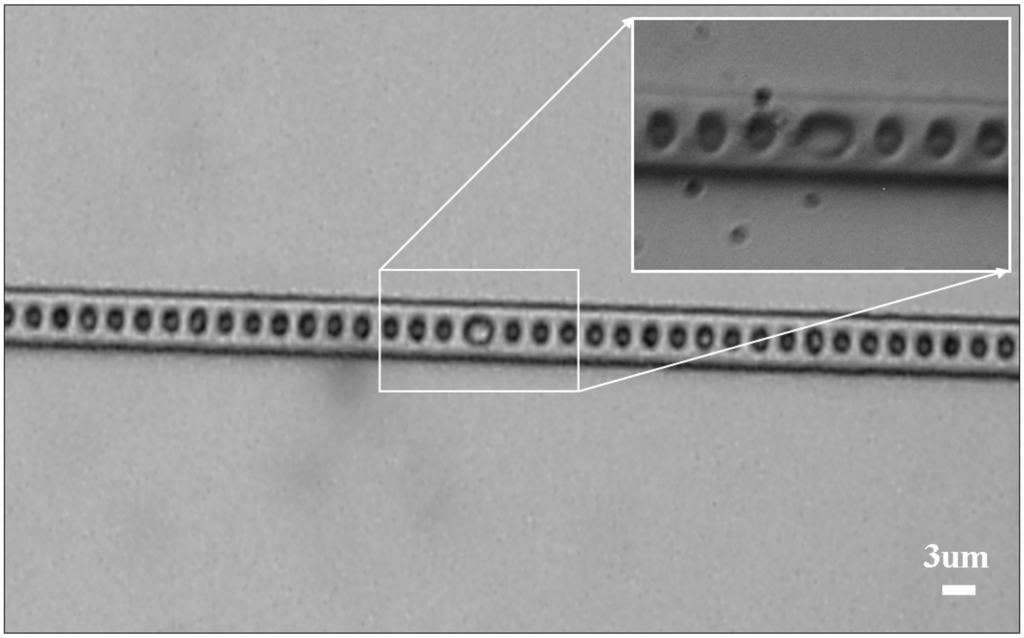

Figure 5.2. Optical micrograph of a microfluidic channel with a 15th order DFB structure on a PDMS chip. The grating period is 3 μm. The central larger PDMS post introduces a 15π phase shift. The inset shows the picture of a real optofluidic dye laser chip.

SU8-2002 negative photoresist (MicroChem) was spin-coated on a silicon wafer and patterned with a Cr-on-glass mask. The mold was treated with tetramethylchlorosilane (Aldrich) for 3 minute before use to facilitate the release of PDMS. Then 5:1 part A:B PDMS prepolymer (GE RTV 615) was poured onto the mold and baked at 80^{o}C for 30 minute. The partially cured PDMS was peeled from the master and the liquid inlet and outlet ports were punched through the whole layer using a 23-gauge luer-stub adapter. This patterned PDMS, containing the laser structure, was then treated with oxygen plasma and bonded to another featureless PDMS to form a monolithic device. Finally, the resulting device was cut to size and baked at 80^{o}C overnight. Figure 5.2 shows an optical microscope image of the central phase shift region of the laser cavity.

5.3 Longitudinal and transverse mode selection

To make a single-mode laser, both the transverse mode and longitudinal mode selection need to be carefully designed. The waveguide dimensions (width 5 μm; height 2 μm) are chosen such that when filled with liquid of refractive index 1.409 it only supports the two fundamental E_{11} modes. If we define the x direction along the width and the y direction along the height, the E_{11}^{x} mode (transverse E field along x direction) is more confined than the E_{11}^{y} mode, and thus is the preferred lasing mode. The small cross-section area also reduces the required pump power to achieve the lasing threshold.

To obtain stable single frequency operation, the free spectral range of the employed cavity structure has to be larger than the gain spectral bandwidth. Organic dye molecules are well known to have very broad gain spectra with a typical bandwidth of 30 nm to 50 nm (full width at half maximum FWHM). This forces the characteristic length of the resonant structure to be shorter than 4 μm. When a DFB structure is used to provide the optical feedback, the lasing wavelength is determined by the Bragg condition:

$$m\lambda_m = 2n_{eff}\Lambda \tag{5.1}$$

where λ_m is the *m*th order resonant wavelength, n_{eff} is the effective index of the guided mode [5] and Λ is the grating period. The free spectral range (*FSR*) is given by:

$$FSR = \frac{\lambda_m}{m-1}, \quad (or \;\; \Delta\nu = \frac{c}{2n_{eff}\Lambda}). \tag{5.2}$$

Therefore for a DFB structure with Λ = 3 μm (1.5 μm + 1.5 μm) and n_{eff} = 1.407, the 15th

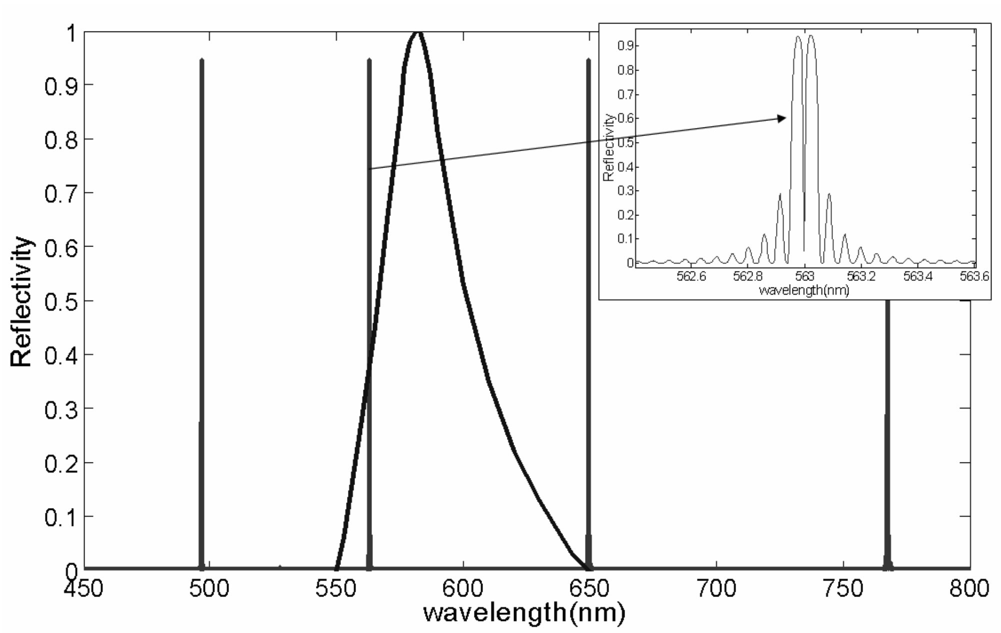

Figure 5.3. Simulated reflectivity spectrum of a 15π phase shifted 15th order DFB structure. The curve spanning from 550 nm to 650 nm is the gain spectrum of Rhodamine 6G. The inset shows the enlarged plot the 15th resonance at 563 nm

resonant wavelength and *FSR* are 563 nm and 40.2 nm respectively. In addition the even order resonances are absent when using a 50% duty-circle square-wave shaped grating. The resulting effective *FSR* of ~ 90 nm ensures a single resonance inside the gain spectrum of Rhodamine 6G which spans from 550 nm to 650 nm. However, within each resonance, there are still side modes, due to the finite length of the grating. It's well known that a DFB laser with a uniform grating operates not at the Bragg wavelength but instead at the two degenerate wavelengths situated symmetrically on either side of the Bragg wavelength [10].

To break this degeneracy, a $14\pi + \pi$ phase shift is introduced at the center of the grating. Figure 5.3 shows the simulated reflectivity spectrum of the overall structure using Rouard's method [11]. The parameters used are: Λ = 1.5 μm + 1.5 μm, grating length L = 4 mm, 15π phase shift at the center, core index n_{core} = 1.409, and cladding/post index n_{clad} = 1.406. It is clearly seen that only the 15th resonance falls in the gain spectrum of Rhodamine 6G. The inset of Figure 5.3 shows the detailed 15th resonance, where the high-pass dip inside the stop band corresponds to the lasing mode.

An interesting property of the higher order DFB structure is that it enables multicolor lasing in the same cavity, each at a single frequency. For example, Figure 5.3 shows that the DFB structure employed in this work can support 497 nm, 563 nm and 650 nm lasing as long as a suitable dye is chosen for each wavelength. This is a highly desired feature for applications where multi-wavelength laser sources are needed, such as multi-color flow cytometry [12] or fluorescence resonance energy transfer (FRET) with multiple donors and acceptors. However, compared with the first order DFB structure, higher order DFB cavities are less efficient in terms of light confinement because the coupling coefficient is inversely proportional to the order of the Bragg scattering [13]. This can be compensated for by increasing the cavity length to provide strong enough feedback.

5.4 Characterization of the dye lasers

The dye solution was introduced into the microfluidic channel by applying 10 psi pressure at the inlet port. We found, to operate the laser in the pulsed mode, it is not necessary to circulate the dye solution. The laser chip was optically pumped with 6 ns Q-switched Nd:YAG laser pulses of 532 nm wavelength, focused to a ~ 100 μm wide stripe aligned with the microfluidic channel. A 10x microscope objective was used to collect the emission light from one edge of the chip and deliver it to a fiber coupled CCD-array based spectrometer with 0.1nm resolution (Ocean Optics HR4000). A typical single mode lasing spectrum is shown in Figure 5.4 where the lasing wavelength is 567.3nm, very close to the predicted value 563nm. The measured linewidth is 0.21nm. A plot of laser output energy

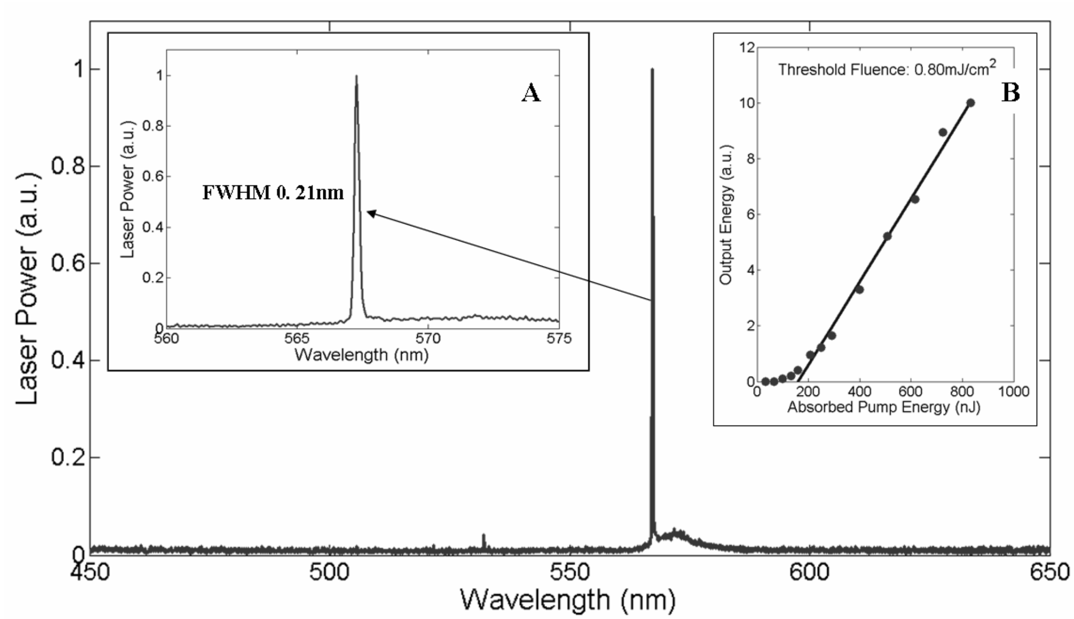

Figure 5.4. Optofluidic DFB dye laser spectrum. The measured linewidth is 0.21 nm. The inset B shows the output energy vs. the absorbed pump energy curve. The threshold pump fluence is ~ 0.8 mJ/cm^2.

versus the absorbed pump energy is shown as the inset B of Figure 5.4. The threshold pump fluence is estimated to be ~ 0.8 mJ/cm^2, which gives peak pump intensity around 150 kW/cm^2. The laser remains single mode at pump levels as high as 8 mJ/cm^2. At moderate pump intensities (200-400 kW/cm^2) and 10 Hz repetition rate, stable laser output lasted longer than 20 minute and the chip can be reused for many times without noticeable degradation.

The elasticity of silicone elastomer and the microfluidics compatibility of the laser chip immediately suggest two wavelength tuning mechanisms. First, the grating period is easily tunable by stretching or compressing the whole chip due to the low Young's modulus of PDMS (~ 750 kPa) [6]. Second, the refractive index of the dye solution can be tuned by mixing two solvents with different refractive indices. For example, using methanol and dimethylsulfoxide (DMSO), the achievable refractive index change can be as large as 0.148 (1.33 for methanol versus 1.478 for DMSO). Furthermore, different dye molecules can be used to cover an even larger spectral range. The mixing, switching and delivery of dye solutions can all be implemented on a silicone elastomer chip using the recently developed mechanical micro valves and pumps [9].

5.5 Conclusion

In this work, we have proposed and demonstrated a phase-shifted 15th order DFB structure as the optical cavity in an optofluidic dye laser system. Single mode operation was obtained with pump fluence from 0.8 mJ/cm^2 to 8 mJ/cm^2. The measured laser linewidth is 0.21 nm. The fabrication and operation of the laser chip is fully compatible with silicone elastomer-based microfluidics technology.

Bibliography

1. Helbo, B., A. Kristensen, and A. Menon, *A micro-cavity fluidic dye laser.* Journal of Micromechanics and Microengineering, 2003. **13**(2): 307-311.
2. Vezenov, D.V., et al., *A low-threshold, high-efficiency microfluidic waveguide laser.* Journal of the American Chemical Society, 2005. **127**(25): 8952-8953.
3. Galas, J.C., et al., *Microfluidic tunable dye laser with integrated mixer and ring resonator.* Applied Physics Letters, 2005. **86**(26).
4. Balslev, S. and A. Kristensen, *Microfluidic single-mode laser using high-order Bragg grating and antiguiding segments.* Optics Express, 2005. **13**(1): 344-351.
5. Coldren, L.A. and S.W. Corzine, *Diode lasers and photonic integrated circuits*. Wiley series in microwave and optical engineering. 1995, New York: John Wiley & Sons. xxiii, 594
6. McDonald, J.C. and G.M. Whitesides, *Poly(dimethylsiloxane) as a material for fabricating microfluidic devices.* Accounts of Chemical Research, 2002. **35**(7): 491-499.
7. Quake, S.R. and A. Scherer, *From micro- to nanofabrication with soft materials.* Science, 2000. **290**(5496): 1536-1540.
8. Xia, Y.N. and G.M. Whitesides, *Soft lithography.* Annual Review of Materials Science, 1998. **28**: 153-184.
9. Unger, M.A., et al., *Monolithic microfabricated valves and pumps by multilayer soft lithography.* Science, 2000. **288**(5463): 113-116.
10. Yariv, A, *Optical electronics in modern communications*. 5th ed. Oxford series in electrical and computer engineering. 1997, New York: Oxford University Press. xviii, 744
11. Wellerbrophy, L.A. and D.G. Hall, *Analysis of wave-guide gratings - application of rouard method.* Journal of the Optical Society of America a-Optics Image Science and Vision, 1985. **2**(6): 863-871.
12. De Rosa, S.C., et al., *11-color, 13-parameter flow cytometry: Identification of human naive T cells by phenotype, function, and T-cell receptor diversity.* Nature Medicine, 2001. **7**(2): 245-248.
13. Streifer, W., D.R. Scifres, and R.D. Burnham, *Coupling coefficients for distributed feedback single-heterostructure and double-heterostructure diode lasers.* IEEE Journal of Quantum Electronics, 1975. **11**(11): 867-873.